Finite Element Method-based Temperature Field Analysis of Early Age Frozen Shaft Lining with Temperature-Dependent Characteristics

Yu Gao[1,2,*], Jie Han[3], Peng Ma[4], Hongguang Ji[1,2] and Chunhui Zhao[5]

[1]School of Civil and Resource Engineering, University of Science and Technology Beijing, Beijing 100083, China
[2]Beijing Key Laboratory of Urban Underground Space Engineering, University of Science and Technology Beijing, Beijing 100083, China
[3]Yankuang Energy(ordos) Co., Ltd, Inner Mongolia 017000, China
[4]Yankuang Energy Group Co., Ltd Ying Pan Hao Coal Mine, Inner Mongolia 017300, China
[5]YU &Associates, inc, NJ 07407, USA

_____

Abstract

Accurately simulating the temperature field of frozen shaft lining in its early age (28 days) is difficult due to the influence of low temperature freezing and the heat of hydration in concrete. The temperature-dependent variation of the thermal properties of concrete and surrounding rock makes the simulation even more challenging. This study proposed a simulation method by considering the concrete maturity to characterize the spatiotemporal variation of temperature field in early age. In accordance with Arrhenius and heat conduction theories, a 3D temperature field control equation containing a model of hydration exothermic with equivalent age was established. The thermal parameters of rock and concrete at different temperatures were obtained through laboratory tests, and the temperature field of the lining was analyzed numerically by using ANSYS Parametric Design Language. The reliability of this method was verified by comparing with the measured data. Comparison results show that the proposed model successfully reflects the facts that the maximum temperature rise at different locations of the lining and the time taken to reach the maximum temperature rise are different. The temperature field in the early age shows five stages: induction period, linear growth period, nonlinear growth period, cooling period, and stabilization period. In the first 3 days, the temperature gradient between the inside and outside of the lining is large, which is prone to early temperature damage. This study provides a significant reference for early temperature damage and lining structure design optimization.

Keywords: Frozen shaft lining, Temperature field, Hydration heat, Equivalent age

_____

1. Introduction

As the "throat" of coal mine production and transportation, the engineering quality of shaft has an important influence on coal mine safety. The freezing method can provide a safe construction environment and stable support conditions for the drilling and ensure the construction quality of the shaft due to the good geotechnical reinforcement and ground water sealing effect. Therefore, the freezing method has gradually become the main technique for the construction of shaft in coal mines with soft and water-rich strata, especially with the Cretaceous and Jurassic strata [1]. However, the increasing depth of shaft leads to the proportional growth of the lining thickness and the amount of cement. Thus, a large amount of hydration heat is released at the early age of the lining and interacts with the freezing temperature to form a large temperature difference inside the lining structure. This large temperature difference results in temperature damage to the lining structure, which affects the quality and service life of the shaft structure. Thus, the study of the developing pattern and distribution characteristics of the temperature field of early-age concrete lining becomes extremely critical for the construction of shaft [2].

Recently, a large number of studies have been conducted on the measurement of temperature changes in frozen shaft and theoretical calculation of temperature fields with numerical analysis techniques. However, the temperature measurement can only be conducted at limited locations due to the complex environment of the deep depth of the shaft. The limited access to measurement hinders the accurate and effective temperature field analysis for quantitatively evaluate the influence of freezing temperature on concrete hydration.

This study establishes a computational model for the early-age temperature field of concrete lining under freezing conditions. With the lab and in-situ tests, we analyzed the concrete hydration and rock thermal parameters under the influence of temperature variation. This process was performed to provide a more accurate characterization of the change pattern and distribution of the early temperature field of the concrete lining and a reference for optimizing the design and construction process of the shaft lining structure.

2. State of the art

At present, scholars have conducted numerous studies, including theoretical models, numerical calculations, field monitoring, and laboratory tests, on the early-age temperature field of concrete structures, such as coal mine shaft, dam and large foundation. Cristian et al. [3] verified the influence of ambient temperature on concrete hydration process and dam temperature field by establishing hydration heat models of concrete dams in adiabatic and nonadiabatic

_____

conditions. However, the range of thermal parameters under different temperatures was not reflected in the analysis. Zhang et al. [4] established a heat conduction equation for the early-age temperature field of mass concrete based on the temperature influence factor and verified the correctness by engineering examples. However, the ambient temperature was set to be constant rather than dynamic in numerical calculations. Klemczak [5] proposed a simple analytical method of temperature field based on transient and nonlinear thermal parameters. This method realizes the prediction of temperature rise and heat exchange of mass concrete floor, but the calculation accuracy needs to be further improved. Smolana et al. [6] conducted finite element analysis of the early temperature field of mass foundations and made recommendations on parameters that can be simplified and focused on in the model, but the effect of ambient temperature on it was ignored in the hydration model. Zhou et al. [7] proposed a mathematical model of the shaft lining temperature field based on the phase change and heat conduction environment of frozen strata and used the finite element method to simulate, but only the phase change latent heat of the strata was considered in the model. Cudowska et al. [8] established a numerical model by using finite difference and finite element method, and realized the time-space description of concrete hydration process under the influence of ambient temperature. However, the influence of thermal parameters on the temperature field under different temperatures was ignored in the analysis. Song et al. [9] used physical model test and finite element numerical simulation to study the early-age temperature rise and distribution characteristics of frozen shaft lining, but the analysis process did not reflect the influence of freezing temperature on the hydration degree of concrete at different positions of shaft lining. Mousavi et al. [10] analyzed the temperature field and the sensitivity of thermal parameters to the temperature field of concrete dam by using a probability model, but lacked the analysis of the influence of ambient temperature on temperature field. Zhang et al. [11] obtained the evolution law of thermal conductivity, specific heat, strength, and elastic modulus of concrete by testing the thermodynamic properties of shaft lining concrete in the first 7 d, but ignored the influence of temperature on the hydration process and the above parameters. Sargam et al. [12] used Concrete Works to predict the thermal property of mass concrete structure in early age and analyzed the sensitivity of different parameters of concrete obtained by laboratory test to the temperature field. However, the applicability of this method in low-temperature environment needs to be verified. Jeong et al. [13] established a mathematical model for the adiabatic temperature rise of concrete based on the chemical reaction of cementitious materials and introduced Arrhenius equation in this model to reflect the influence of ambient temperature on hydration rate. However, the relevant data under negative temperature conditions were missing in the validation test. Do et al. [14] established a concrete hydration exothermic model based on

the equivalent age through adiabatic temperature rise test of conventional concrete and high-strength concrete, and applied it to the finite element analysis of the early temperature field of bridge pier structure. However, the other thermal parameters in the analysis were taken as constant values, which did not correspond to the actual situation. An et al. [15] established a real-time prediction method for the early temperature of concrete dams based on field monitoring data and presented a hydration temperature rise rate equation, which is only dependent on monitoring data and can only predict the temperature at the monitoring point. Zhang et al. [16] conducted an in-situ measurement study on the temperature development pattern of mass high-performance concrete shaft lining and fitted a double exponential relationship between temperature rise and age. However, only a few layers can be studied because of the limitation of the number of measurement points.

The above exploration results are mainly for the temperature field of the mass concrete structure under normal temperature conditions above ground, and studies on the mass high-strength concrete structure in the low-temperature environment of underground projects are few, especially the hydration process of concrete under low-temperature environment and its influence on the temperature field is rare. This study establishes 3D temperature field control equations containing hydration exothermic model with equivalent age based on Arrhenius and heat conduction theories, obtains thermal parameters of sandstone and concrete at different temperatures through laboratory tests, and analyzes the early temperature field variation law and distribution characteristics of lining by using ANSYS Parametric Design Language (APDL), which provides reference for the structure and material design and construction process optimization.

The remainder of this study is organized as follows. Section 3 builds a temperature field calculation model, and conducts concrete adiabatic temperature rise and thermal parameter tests at different temperatures. Section 4 analyzes the early-age temperature field of the frozen shaft lining by using the finite element analysis method. Section 5 provides the conclusions.

3. Methodology

3.1 Engineering background
This study takes the auxiliary shaft of Erdos Yingpanhao Coal Mine in China as the research object. This shaft is a double-layer structure, and its designed diameter is 10.0 m. The research location crosses the Cretaceous strata, with fine sandstone predominantly, and the thickness of the inner lining is 1.15 m, using C60 concrete, and the thickness of the outer lining is 0.4 m, using C50 concrete. The actual proportions of the two types of concrete are shown in Table 1.

Table. 1. Shaft lining concrete mix proportion with different strength grades($kg \cdot m^{-3}$)

Concrete strength grade	Water–cement ratio	Cement	sand	Gravel	Water	High-performance concrete admixture	Cement type	Density
C50	0.33	421	718	1122	139	37.91	P.O 42.5R	2437
C60	0.32	419	720	1127	134	50.25	P.O 52.5R	2450

Temperature sensors were installed inside the structure, which monitored the temperature data of 28 days after pouring to obtain the pattern of temperature development and verify the validity of the proposed calculation model.

3.2 Theoretical model
Temperature field describes the temperature of all points in the space at different times, which is a function of time and space coordinates.

$$T = f(x, y, z, \tau) \tag{1}$$
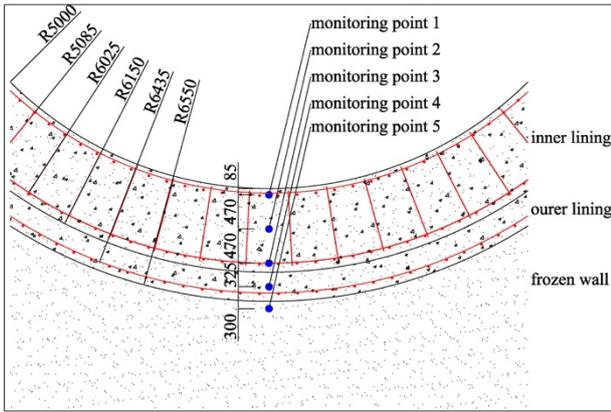
Fig. 1. Distribution of temperature sensors

The heat transfer mechanism of the temperature field in frozen shaft area is shown in Fig. 2. It includes concrete hydration heat, constant temperature boundary, heat conduction boundary, and thermal convection boundary.
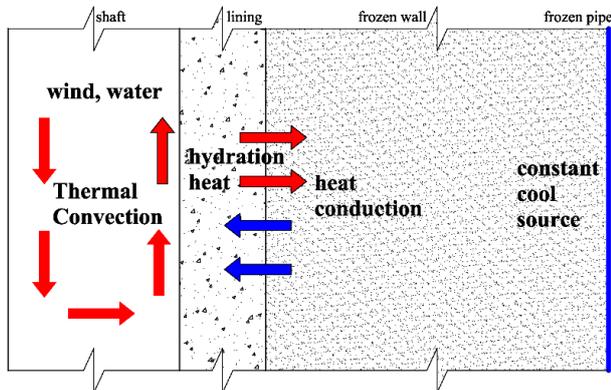
Fig. 2. Heat transfer mechanism for the temperature field of frozen shaft

Inside the structure, the temperature field changes constantly due to heat conduction. The essence of heat conduction is the change and transfer of heat flow inside the structure. Fourier derived from experimental analysis that the density of heat flow transmitted along the isothermal (surface) normal direction is proportional to the temperature gradient, and the expression is shown in Eq. 2.

$$q = -\lambda \frac{\partial T}{\partial n} \tag{2}$$

For concrete structures, the adiabatic temperature rise caused by the heat release of hydration can be expressed as

$$T(t) = \frac{m \cdot Q(t)}{c\rho} \tag{3}$$

where c is the specific heat capacity of concrete, J/(kg·°C); ρ is the concrete density, $kg \cdot m^{-3}$; $Q(t)$ is the heat released per unit volume of concrete at time t, $J \cdot m^{-3}$; m is the cement consumption per unit volume, $kg \cdot m^{-3}$.

High-strength concrete produces a large amount of hydration heat in the early stage. As a thermal conductive solid, its Fourier law of thermal conductivity must be

changed accordingly. In accordance with the principle of energy conservation, the volumetric heat balance that must be satisfied at each point inside the lining, that is, the heat absorbed or released by the change in temperature inside the concrete is equal to the sum of the heat flow and its internal heat of hydration. It describes the dependence of the temperature in the solid on the spatial coordinates and time, that is, the controlling equation of the temperature field of the concrete structure.

$$\frac{\partial T}{\partial t} = \frac{\lambda}{\rho c}\left(\frac{\partial^2 T}{\partial x^2} + \frac{\partial^2 T}{\partial y^2} + \frac{\partial^2 T}{\partial z^2}\right) + \frac{q(t)}{\rho c} \tag{4}$$

where ρ is the material density, $kg \cdot m^{-3}$; c is the specific heat of material, J/(kg·°C); λ is the thermal conductivity of material, J/(m·h·°C); $q(t)$ is the hydration heat per unit volume and unit time, $J/(h \cdot m^{-3})$.

Here, the specific values of ρ, c, and λ for concrete and fine sandstone need to be obtained experimentally. c and λ vary with the ambient temperature, especially in the presence of water inside. Therefore, the study was conducted to determine the thermal conductivity and specific heat capacity of sandstone and concrete specimens at −30 °C to 30 °C and 0 °C to 90 °C by using a Hot Disk TPS 2500S thermal constant analyzer based on the transient planar heat source technology. The test equipment is shown in Fig. 3.

Fig. 3. Hot Disk TPS 2500S Thermal Constant Analyzer

Eq. 4 establishes the spatiotemporal relationship of the temperature in the shaft area, but the initial and boundary conditions need to be given to solve for the actual temperature field.

The initial condition is the temperature distribution at the initial moment of the temperature field. Considering that the frozen shaft engineering area is under the influence of ventilation, water, and freezing temperature, its initial temperature distribution is a certain function related to space rather than a constant.

$$T_0 = T(x, y, z, t = 0) \tag{5}$$

The formation of the frozen wall is formed by continuously freezing the surrounding rock mass with low-temperature brine inside the frozen pipe. Thus, the frozen brine temperature can be used as a constant cold source boundary condition in the study of the temperature field.

$$T_{(r=l_p)} = t_b \tag{6}$$

where t_b is the temperature of the brine in the frozen pipe, °C; l_p is the distance from the frozen pipe to the center of the shaft.

The heat conduction boundary conditions are between the upper and lower sections of the shaft lining and between the shaft lining and the frozen wall. Assuming that the contact surface is in good contact, we have

$$-\lambda_1 \frac{\partial T_1}{\partial n} = f(t) = -\lambda_2 \frac{\partial T_2}{\partial n} \tag{8}$$

where λ_1 and λ_2 are the thermal conductivities of the two contacting solids.

The thermal convection boundary condition exists between the surface of the lining and the air or water surrounding the shaft. Its strength depends on the temperature difference between the surface and the fluid. Convective heat transfer can be expressed by the classical Newton's law of cooling.

$$q(t) = h_c[T_s(t) - T_a(t)] \tag{8}$$

where q is the unit area heat flow rate, W/m^2; h_c is the convective heat transfer coefficient, W/(m$^2 \cdot$ °C); T_s is the concrete surface temperature, °C; T_a is the flowing air temperature, °C.

The convective heat transfer coefficient h_c depends mainly on the roughness of the concrete surface and the thermal conductivity, viscosity coefficient, and wind speed of the flowing air.

3.3 Hydration heat model
The actual state of the cement hydration reaction can be described by the degree of hydration, which is defined as the ratio of the amount of cement hydrated at moment t to the amount of original cement in the mix. Considering that the essence of the hydration reaction is exothermic, the degree of hydration can also be defined as the ratio of the accumulated heat $Q(t)$ released per unit mass of cement hydration time t to the total heat Q_0 released after complete hydration.

$$\alpha(t) = \frac{Q(t)}{Q_0} \tag{9}$$

The relationship between the hydration degree and the adiabatic temperature rise can be obtained by substituting Eq. 3 into Eq. 9.

$$\alpha(t) = \frac{Q(t)}{Q_0} = \frac{T(t)}{T_0} \tag{10}$$

The curve of adiabatic temperature rise versus time can be expressed in exponential form.

$$T(t) = T_0 \left[1 - \exp(-at^b)\right] \tag{11}$$

where a and b are the time and shape parameters of the adiabatic temperature rise curve obtained by fitting.

The temperature rise curve is obtained by the adiabatic temperature rise test. The test uses the BY-ATC/JR concrete

adiabatic temperature rise tester jointly developed by the China Academy of Building Sciences and Zhoushan Boyuan Science and Technology Development Co., Ltd., as shown in Fig. 4. The adiabatic temperature rise curve obtained by the experiment is fitted by using Eq. 11, and the composite exponential form of adiabatic temperature rise is obtained.

Fig. 4. BY-ATC/JR concrete adiabatic temperature rise tester

The hydration expression based on the adiabatic temperature rise test is obtained by bringing Eq. 11 into Eq. 10.

$$\alpha(t) = 1 - \exp(-at^b) \tag{12}$$

Considering that the hydration environment of concrete in early-age frozen shaft lining is different from the adiabatic temperature rise test conditions in the laboratory, the influence of environmental temperature on the hydration process should be considered when calculating the hydration heat release of concrete cement in the field. Maturity theory is used to consider the influence of temperature and time on its hydration process comprehensively, and a maturity function based on equivalent age is established to convert the concrete maturity under variable temperature conditions into equivalent concrete curing time and relate it to the temperature function. Eq. 13 denotes the time required for concrete cured at reference temperature T_e to reach the same performance as concrete cured at variable temperature T at moment t.

$$t_e = \int_{t_0}^{t_t} \exp\left[\frac{E_a}{R}\left(\frac{1}{293} - \frac{1}{273 + T_t}\right)\right] dt \tag{13}$$

where R is the gas constant, which is usually 8.314 J/mol/°C; E_a is the activation energy of cement hydration, which is 37.2×10^3 J/mol; T_t is the average temperature inside the concrete at the moment t, °C.

Substituting Eqs. 10 and 13 into Eq. 12 can obtain the heat of hydration at a given age time.

$$Q(t) = Q_0 \cdot [1 - \exp(-at_e^b)] \tag{14}$$

The exothermic rate of hydration per unit volume of concrete in time t can be obtained by deriving Eq. 14.

$$q(t) = Q_0 \cdot a \cdot b \cdot t_e^{b-1} \cdot \exp(-a \cdot t_e^b) \cdot \exp\left[\frac{1}{R}\left(\frac{E_a}{293} - \frac{E_a}{273 + T_t}\right)\right] \tag{15}$$

The combination of Eqs. 4 to 8 and Eq. 15 forms the final temperature field calculation model.

3.4 Geometric model and basic assumptions

To preserve population diversity after the particle position has been updated, we have designed a turbulence operator. In the process of Ansys analysis of the early temperature field of frozen deep draft, a systematic analysis of the freeze-hydration interaction process needs to be conducted in conjunction with the construction conditions. The original temperature field of the formation formed a new stable temperature field due to the freezing effect before the lining was poured, so a steady-state thermal analysis calculation was needed for the wellbore area, which formed a heat load distribution that did not change with time. When the lining starts pouring, transient thermal analysis is needed on the basis of the above stable temperature field because the hydration reaction is a dynamic process. During the analysis, the heat generated by the hydration reaction and the convection and heat transfer between the surface of the lining and the air and frozen wall temperatures need to be considered to determine the response of the temperature field with time. Combining the contents of Sections 3.1 to 3.3, an early temperature field analysis program for frozen shaft lining was prepared on Ansys APDL, and the following assumptions were made.

(1) The material of the lining and the frozen wall are each identical and homogeneous, and no gap is observed between all types of materials with complete contact.

(2) Ignoring the effect of excavation diameter, the model of the shaft is built exactly in accordance with the design dimensions.

(3) The effects of reinforcement, steel fiber material, and metal formwork on thermal parameters are considered in the material properties in the model rather than modeling the reinforcement and metal formwork.

(4) In the layered casting, the casting time is assumed to be completed instantaneously, the height of the casting section is 1.2 m, and the casting interval of each layer is 3 h.

(5) The effect of water in the rock formation on the temperature field of the shaft when the frozen wall melts is ignored.

(6) The calculated model has the same temperature load in all directions, which can be simplified to a symmetric model.

4 Result Analysis and Discussion

4.1 Parametric analysis

The maximum temperature rise of C60 concrete and the temperature rise curve can be obtained through the adiabatic temperature rise test. The values of parameters a and b can be obtained by fitting the test data through Eq. 11, and the final heat release amount Q_0 can be obtained through Eq. 3. The hydration heat release model based on equivalent age can be obtained by substituting a, b, and Q_0 into Eq. 15. From the test, the concrete finished the hydration exotherm at 24 h, and the maximum temperature rise reached 53.09 °C.

$$q_{C60}(t) = 7.7 \times 10^3 \times t_e^{2.12} \exp(-9.68 \times t_e^{3.12})$$
$$\times \exp[4.47 \times 10^3 \times (\frac{1}{293} - \frac{1}{273 + T_t})] \quad (16)$$
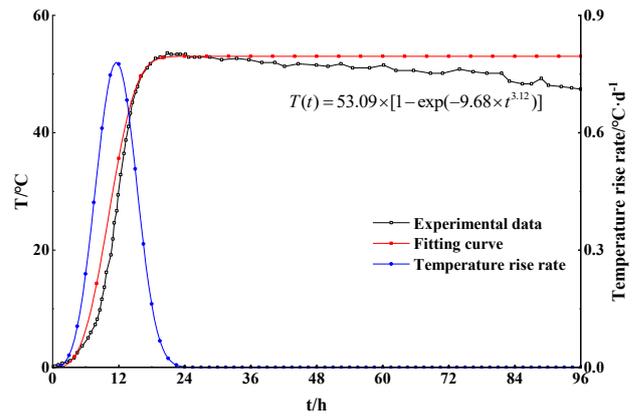
Fig. 5. Adiabatic temperature rise curve of C60 concrete

$$T(t) = 53.09 \times [1 - \exp(-9.68 \times t^{3.12})]$$
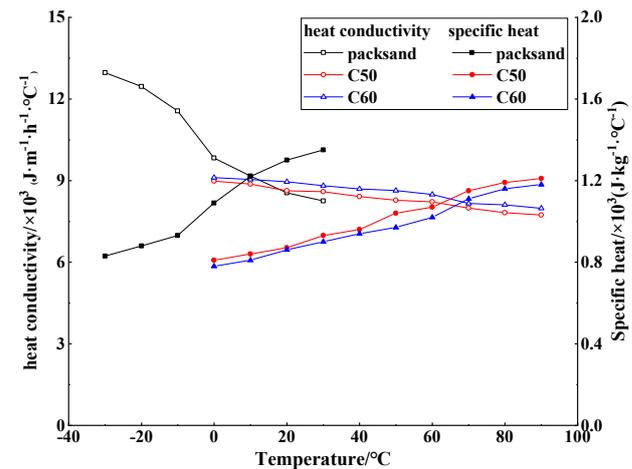
Fig. 6. Thermal conductivity and specific heat of specimens at different temperatures

The thermal conductivity and specific heat of fine sandstone and concrete specimens at different temperatures were obtained by transient planar heat source tests. As shown in Fig. 6, the thermal conductivity and specific heat of fine sandstone are more sensitive to temperature. With the increase in temperature, the solid ice in the pores of the sandstone gradually thaws into liquid water, which makes the thermal properties vary more in the range of −10 °C–10 °C. Overall, the effect of temperature on the thermal properties of the two specimens cannot be ignored.

4.2 Model verification

From Fig. 7, the calculation results of the modified model with equivalent age hydration exotherm can be more realistic than those of the conventional hydration exotherm model, which are mainly reflected as follows:

The maximum temperature rise is different at different locations of the lining. Considering that the boundary conditions inside, middle, and outside of the lining lead to different heat transfer, different degrees of temperature rise are observed at different locations. However, the comparison between the two models and the measurement data shows that the degree of hydration at different locations needs to be considered. Given that the actual ambient temperature on the inside and the outside of the lining is less than the standard curing temperature, the concrete in this region cannot be fully hydrated, resulting in different maximum temperature rise at different locations of the lining (outside < inside < central ≈ adiabatic temperature rise test). The calculation results using the equivalent age hydration exothermic

correction model are closer to the actual measured temperature.

The time taken for the maximum temperature rise differs at different locations of the lining. From the measured temperature, the time taken for the maximum temperature rise of the lining shows the state of inner < central < outer, and the calculation results using the conventional hydration exothermic model show a basic agreement. The analysis shows that the inner side of the lining remains stable due to ventilation, and its hydration process is stable. On the outer side of the lining, its ambient temperature (outer lining, frozen wall) increases remarkably due to the heat of hydration, and the change in ambient temperature affects the hydration process of concrete in this area. The use of the equivalent age hydration exothermic correction model can effectively reflect the above phenomenon and more accurately describe the changes in the early temperature field of the frozen shaft lining.
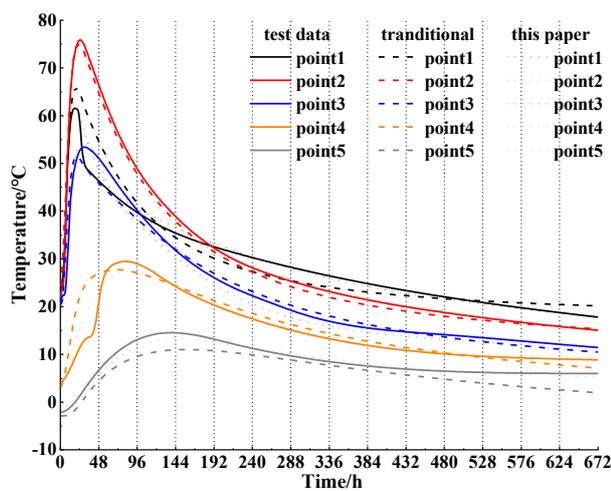
Fig. 7. Variation of temperature with time
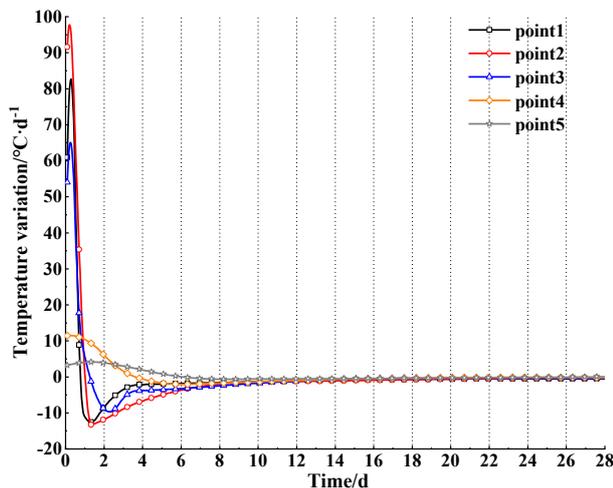
Fig. 8. Temperature variation rate

4.3 Development of temperature field
In accordance with Figs. 7–8, the early change pattern of the lining temperature field can be obtained, which is mainly divided into five stages.

Phase 1 (induction period): The temperature change 1–2 h after pouring is unremarkable that is, the temperature of concrete into the mold. The internal hydration product has not formed effective diffusion, the reaction rate is slow, and is in the induction stage of hydration process.

Phase 2 (linear growth period): The temperature change starts to enter the linear growth period when the hydration reaction is intense after the induction period, releasing a large amount of heat and causing the temperature of the shaft lining to rise rapidly. The temperature growth rate of measurement points 1 and 2 reached 2.3 °C/h, and measurement point 3 was 1.2 °C/h.

Phase 3 (nonlinear growth period): At this time, the temperature growth rate decreases with the increase in temperature until the peak temperature. The degree of hydration and the maximum temperature rise in different locations in the lining varied in this stage, showing the highest temperature rise in the middle, reaching 75.8 °C, followed by the inside, reaching 61.5 °C, and the outside, reaching 53.4 °C. This finding indicates that the ambient temperature has a temporal and spatial influence on the hydration process of concrete.

Phase 4 (cooling period): The internal temperature of the lining decreases in an approximate power function curve after about 1 d of the hydration reaction because decreasing heat is released, and the external ambient temperature begins to play a dominant role.

Phase 5 (stabilization period): The cooling rate gradually stabilizes after about 14 d, at which point the ambient temperature and the thermal properties of the lining material are constant, allowing the temperature to vary in an extremely small interval.

4.4 Spatial distribution of temperature field and temperature gradient
Figs. 9–10 show the radial distribution of shaft temperature and temperature gradient at different times. From Fig. 12, the temperature of the lining showed central > inner > outer at the early stage, especially before 7 d, and the temperature difference between the central and outer > the temperature difference between the central and inner, with the maximum temperature difference of 32.7 °C. As shown in Fig. 13, the temperature gradient of the inner and outer is extremely large due to the influence of the ambient temperature, especially the outer, where its temperature gradient exceeds 100 °C/m in 3 d. Subsequently, the change value of the temperature gradient in the inner and outer decreases remarkably.
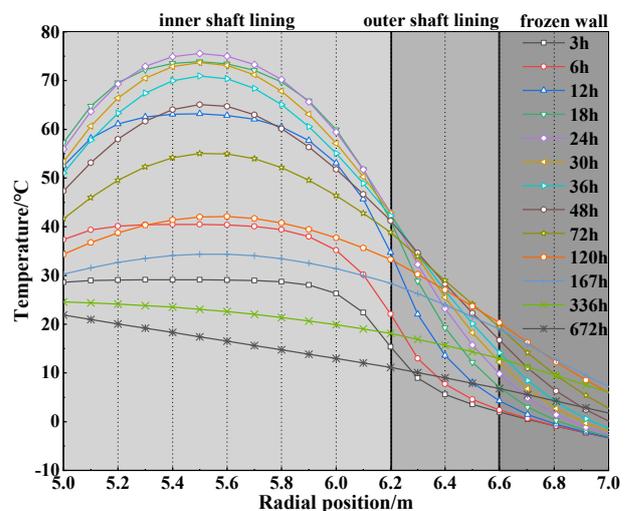
Fig. 9. Radial distribution of temperature

Comprehensive analysis on the development law and spatial distribution characteristics of the lining temperature field shows that within 3 d after the concrete is poured. The

temperature gradient at the inner and outer edges of the lining is large, and the temperature change rate is high, which is easy to produce obvious early temperature stress, especially when the concrete strength has not reached the design strength. The temperature stress easily leads to the generation of cracks in the lining when it exceeds the strength of the lining concrete.
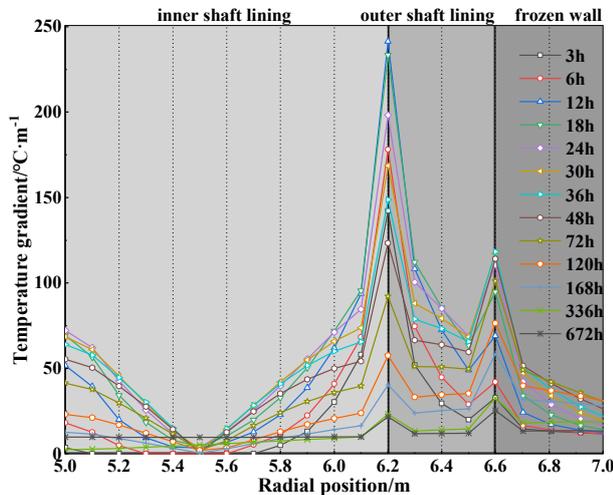
Fig. 10. Radial distribution of temperature gradient

5. Conclusions

A 3D temperature field control equation containing an equivalent age hydration exothermic model based on Arrhenius and heat conduction theories was established to reflect the influence of ambient temperature on the hydration heat of concrete in the numerical analysis and to precisely investigate the development characteristics of the early temperature field of the lining under the freeze-hydration effect. The early temperature change pattern and spatial distribution characteristics were analyzed by using laboratory tests and finite element analysis techniques. The conclusions are summarized as follows:

(1) The thermal parameters of fine sandstone and concrete vary greatly at different temperatures, especially near 0 °C, which should be considered in the simulation of temperature field.

(2) The proposed model more accurately reflects the variation pattern of the early temperature field in time and space, and reveals the actual situation that the maximum temperature rise at different locations on the lining and the time taken to reach the maximum temperature rise are different.

(3) The development of temperature field in the early age (28) showed five stages: induction period, linear growth period, nonlinear growth period, cooling period, and stabilization period. The maximum temperature rise occurred in the middle of the lining, reaching 75.8 °C at 20 h.

(4) The maximum temperature difference in the lining structure appears between the middle and the outside, reaching 32.7 °C, and the temperature gradient in the inside and outside of the lining is large in the first 3 d, which is easy to produce early temperature damage, and relevant measures should be taken during construction.

In this study, the concept of hydration equivalent age is introduced into the numerical analysis of the early temperature field of frozen shaft in coal mines, which reflects the influence of temperature on the hydration heat and thermal properties of concrete. The analysis results are more suitable for the actual situation in the field, which provides a certain basis for the subsequent study of early temperature damage of the lining and the optimization of the lining structure design. However, the material thermal parameters in the model are taken discontinuously, and only the material thermal parameters at some temperatures are studied experimentally. Thus, the results of the simulated temperature field will be more accurate in future research by establishing the relationship between the temperature and material thermal parameters.

References

1. Yao, Z. S., Cheng, H., Rong, C. X., "Shaft structural design and optimization of deep freezing bedrock shaft in west area". *Journal of China Coal Society*, 35(5), 2010, pp.760-764.
2. Liu, X. H., Zhou, C. B., Chang, X. L., "Simulation of mass concrete temperature cracking propagation process". *Rock and Soil Mechanics*, 31(8), 2010, pp. 2666-2676.
3. Ponce-Farfán, C., Santillán, D., Toledo, M. Á, "Thermal Simulation of Rolled Concrete Dams: Influence of the Hydration Model and the Environmental Actions on the Thermal Field". *Water*, 12(3), 2020, pp. 858.
4. Zhang, M., Yao X. H., Guan J. F., Li L. L., "Study on Temperature Field Massive Concrete in Early Age Based on Temperature Influence Factor". *Advances in Civil Engineering*, 2020, pp. 8878974.
5. Klemczak B., "Analytical Method for Predicting Early Age Thermal Effects in Thick Foundation Slabs". *Materials*, 12(22), 2019, pp. 3689.

6. Smolana A., Klemczak B., Azenha M., Schlicke D., "Thermo-Mechanical Analysis of Mass Concrete Foundation Slabs at Early Age Essential Aspects and Experiences from the FE Modelling". *Materials*, 15(5), 2022, pp. 1815.
7. Zhou, X. M., Guan, H. D., Zhang, L.，"Temperature field research of mass concrete based on the phase change condition of ground freezing wall". *Journal of Basic Science and Engineering*, 25(2), 2017, pp. 395-406.
8. Aleksandra, K. C., Krzysztof, W., "FEM and experimental investigations of concrete temperature field in the massive stem wall of the bridge abutment", *Construction and Building Materials*, 347, 2022, pp.128565.
9. Song, H. Q., Cai, H. B., Cheng, H., Yao, Z. S., "Physical model testing and numerical simulation for temperature distribution of mass concrete freezing shaft lining in deep alluvium", *AIP Advances*. 8, 2018, pp.075328.
10. Seyed, M. M., Majid, P. K., "Thermal Analysis of Roller Compacted Concrete Dam Utilizing a Probabilistic Model". *Mathematical Problems in Engineering*, 2022, pp.3781989,.

11. Zhang, C., Zhang, Y., Yang, W., Yin, J., Zhang, T., "Study on Evolution of the Thermophysical and Mechanical Properties of Inner Shaft Lining Concrete during Construction Period". *Applied Sciences*, 12(19), 2022, pp. 10141.

12. Sargam, Y., Faytarouni, M., Riding, K., Wang, K. J., Jahren, C., Shen, J., "Predicting thermal performance of a mass concrete foundation – A field monitoring case study", *Case Studies in Construction Materials*, 11, 2019, pp. e00289.

13. Jeong, D. J., Kim, T., Ryu, J. H., Kim, J. H., "Analytical model to parameterize the adiabatic temperature rise of concrete". *Construction and Building Materials*, 268, 2021, pp. 121656.

14. Do, T. A., Hoang, T. T., Thanh, B. T., Hoang, H. V., Do, T. D., Nguyen, P. A., "Evaluation of heat of hydration, temperature evolution and thermal cracking risk in high-strength concrete at early ages", *Case Studies in Thermal Engineering*, 21, 2020, pp. 100658.

15. An, G., Yang, N., Li, Q., Hu, Y., Yang, H., "A Simplified Method for Real-Time Prediction of Temperature in Mass Concrete at Early Age". *Applied Sciences*, 10(13),2020, pp. 4451.

16. Zhang, T., Yang, W. H., Chen, G. H., "Monitoring and analysis of hydration heat temperature field for high performance mass concrete freezing shaft lining". *Journal of Mining & Safety Engineering*, 33(2), 2016, pp. 290-296.